

Attitude Control System Design for Return of the Kistler K-1 Orbital Vehicle



David S. Rubenstein
David W. Carter

Winner of Draper's 1998 Best Paper Award

© 1998 AIAA. Reprinted, with permission, from the Collection of Technical Papers of the AIAA Guidance, Navigation, and Control Conference and Exhibit, Boston, MA, 10-12 August 1998, pp. 1410-1422

Kistler K-1 Orbital Vehicle: Photo Credit - Kistler Aerospace Corporation

ABSTRACT

The Kistler K-1 vehicle is an unmanned reusable launch system that is intended to deliver payloads to low Earth orbit and return to Earth, landing within a designated target radius and in a condition conducive to rapid turnaround for reuse up to 100 times with a minimum of maintenance and preparation. The vehicle consists of two stages, the first-stage Launch Assist Platform (LAP) and the second-stage Orbital Vehicle (OV). The LAP lifts the combined stack to an altitude from which the OV can achieve the necessary orbital conditions and then returns to the landing site, landing with parachutes and airbags. After achieving orbit and deploying the payload, the OV reenters the atmosphere and, using active guidance and control, negotiates the required maneuvers to attain a trajectory that will result in a safe and accurate return to the landing site, and also lands with parachutes and airbags. The attitude control system (ACS) responds to commands from the guidance system by constructing and executing bank maneuvers to strategically rotate the lift vector. In addition, the control system must monitor and maintain various aerodynamic conditions associated with performing effective and efficient banks. This paper presents the approach to bank maneuver construction, aerodynamic parameter maintenance and estimation philosophies and design, and application of the phase plane control concept to the atmospheric reentry problem.

INTRODUCTION

The K-1 OV attitude control system is responsible for controlling the vehicle from shortly after the deorbit burn through atmospheric reentry and landing under the OV main parachute system. The control system consists of three main modes of operation to accommodate the unique requirements for the different mission phases. The Entry Control (EC) mode is the primary mode of operation and is active from just beyond deorbit (when handover from the OV on-orbit control system occurs) through atmospheric reentry. The EC mode is terminated on deployment of the OV stabilization parachute. This action is triggered by a Mach number threshold (likely in the vicinity of 2.6). The primary role of the EC mode is the intelligent construction and execution of coordinated bank-

about-velocity commands from the OV entry guidance system required to return the vehicle safely to the target landing zone.

In addition, during EC, the control system will monitor and maintain critical aerodynamic parameters necessary for efficient and effective banks. An aerodynamic estimator, which estimates the current trim conditions for the OV, provides EC with additional information necessary to precisely maintain the desired lifting characteristics on the vehicle.

The other modes in which the controller operates are the Yaw-to-Velocity (YC) mode, which is responsible for reorienting the OV while under the main parachute system such that the vehicle longitudinal axis is aligned with the Earth relative velocity direction; and the Monitor-for-Yaw (MC) mode, which simply monitors vehicle states to determine if it is time to transition to the YC mode. The MC mode produces no attitude control commands. The YC mode is intended to ensure that the OV can land safely on the landing airbag system.

This paper is concerned only with the EC mode of the controller. It describes the basic technical approach for EC maneuver construction and control as well as the approach to aerodynamic estimation. Flow diagrams and figures are presented to clarify design and implementation. Results are presented for a set of nominal simulations run using the Draper Laboratory K-1 Integrated Vehicle Simulation (IVS).

ATTITUDE CONTROL SYSTEM DESIGN

EC is the primary mode of the OV return attitude control system. It is active for the longest period of time, from just beyond deorbit burn through the terminal guidance mode responsible for computing the constant bank angle to minimize the final horizontal target miss of the OV. The EC mode constructs and executes the desired bank-about-velocity maneuvers, and monitors and maintains the necessary aerodynamic conditions. In order to accomplish these tasks, EC must perform several critical activities:

1. Compute current actual aerodynamic bank, side-slip, and angle-of-attack (ϕ , β , α).

2. Perform aerodynamic estimation to provide information needed for efficient control. These include the current trim angle of attack (α_{trim}), the characteristic frequency of the angle-of-attack oscillations (Ω), and the amplitude of these oscillations (A).
3. Compute the current Euler coupling accelerations ($\ddot{\theta}_{cc}$).
4. Determine the correct (signed) delta-bank ($\Delta\phi$) maneuver to accomplish the guidance command.
5. Compute the rotational rates of the air-relative velocity vector and the bank vector.
6. Construct the appropriate rotation vector for the bank maneuver.
7. Determine the necessary correction for side-slip maintenance.
8. Compute the current angle and rate errors associated with the current vehicle state. (For banks/side-slip control, this will include only the roll and yaw axes.)
9. Determine the appropriate control action for the bank based on these errors, using a phase plane control implementation.
10. Determine the appropriate pitch-axis command based on information from the estimator and the vehicle state.
11. Generate the necessary ACS jet selection vector from a simple look-up table, based on the desired control actions.

The EC controller requires various inputs from several sources. In particular, the OV navigation function provides:

1. Current position vector in the inertial reference (\vec{r}_i).
2. Current inertial velocity in the inertial frame (\vec{V}_i).
3. Current inertial-to-body attitude quaternion (\vec{q}_{ib}).
4. Current inertial angular rate in the OV body frame ($\vec{\omega}_B$).
5. Current aerodynamic force in the inertial frame (this is estimated using sequential "sensed velocity" measurements compensated for ACS jet forces) (F_{aero}).

The OV guidance function provides:

1. Current vehicle commanded aerodynamic bank angle (ϕ_c).
2. Current vehicle commanded bank rate ($\dot{\phi}_c$).

The OV EC initialization function provides:

1. Jet force and torque vector from previous cycle (F_{jets} , N_{jets}).
2. An estimate of the current aerodynamic force (F_{aero}).

The primary responsibility of EC is to execute these commands from guidance in an expedient and (fuel) efficient

manner, using the inputs from navigation. The primary EC outputs are the vector of selected ACS jets to bring about the desired control action (\vec{J}), a flag indicating whether a particular bank maneuver has completed, and the current bank angle. The EC controller, then, can be categorized in three main functions:

1. Computation of aerodynamic angles and aerodynamic estimation.
2. Bank maneuver/side-slip construction and control.
3. Pitch-axis control (angle-of-attack oscillation maintenance).

These are discussed in detail below.

AERODYNAMIC ANGLES AND ESTIMATION

Overview

In order to perform its various functions, reentry control requires current values of the vehicle angle of attack (α), the side-slip angle (β), and the bank angle (ϕ^*). To damp the natural oscillation in angle of attack, estimates of the trim angle of attack (α_{trim}) and estimates of the α -oscillation amplitude and frequency are also needed. The design of the reentry controller includes a capability to compute these quantities. Figure 1 shows the architecture of this capability.

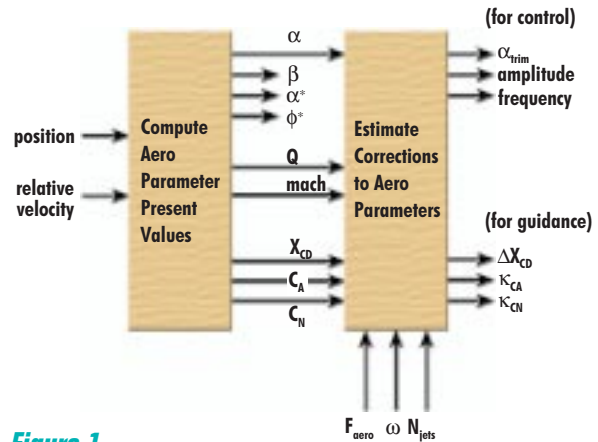


Figure 1

Aerodynamic parameter estimation

Current Values of Aerodynamic Angles

Angle of attack (α), side-slip angle (β), and total angle of attack (α^*) are related to v_{air} , the vehicle velocity with respect to the atmosphere expressed in body coordinates, as follows

$$(1) \quad v_{air} = \|v_{air}\| (\cos \alpha^*, \sin \beta, \sin \alpha)$$

The design uses this relation to obtain α , β , and α^* . A pre-stored wind profile is used to obtain velocity with respect to the atmosphere from navigated velocity with respect to earth. The determination of α , β , and α^* thus involves two main sources of error:

1. The Enhanced GPS INS (EGI) instrument used for navigation is aligned imperfectly. Thus, the body coordinates of velocity with respect to Earth may be incorrect.
2. Winds are only crudely modeled.

EGI alignment to within ± 1.0 deg is specified. Note that EGI misalignment errors will be essentially constant over the short time (less than 15 min) that reentry control is active. We talk further about bias errors below.

To estimate the error introduced by mismodeling wind, 400 reentry trajectories were simulated using randomly seeded Gram-95 atmosphere and wind modeling. The wind velocity vector was averaged over each simulated trajectory, and the distribution of the average wind vectors was examined. By this method, it was found that the average crosswind speed can be expected to be approximately 90 ft/s (1σ). Keeping in mind that the vehicle speed exceeds Mach 10 for almost all the trajectory, the average angular error that we would incur by *neglecting* wind will be on the order of an arctangent of 0.01, i.e., on the order of 0.5 deg (1σ). By using a wind profile, we hope to incur smaller errors.

The vehicle bank angle (ϕ^*) is, by definition, the angle between two planes, namely:

1. The plane spanned by the velocity vector and the inertial position vector (the vertical plane).
2. The plane spanned by the velocity vector and the vehicle longitudinal (x) axis.

We compute the angle between these planes as the angle between their normal vectors, which are obtained, respectively, as follows:

1. The cross product of the air velocity vector with the navigated position vector.
2. The cross product of the air velocity vector with the vehicle x axis.

Note that the dominant source of error in computed ϕ^* is EGI misalignment.

Current Values of Dynamic Pressure and Mach Number

The simplest approach is felt to be adequate: the design uses prestored tables of atmospheric density (ρ) and speed of sound (v_{sound}); each is parametrized by altitude (h). The two tables are provided to the flight system as part of the "mission load" database.

Vehicle altitude is determined by navigation. Atmospheric density (ρ) and speed of sound (v_{sound}) are then found by linear interpolation in the respective tables.

Dynamic pressure Q and Mach number m are computed from ρ , v_{sound} , and $\|v_{\text{air}}\|^2$ in the obvious way

$$Q = \frac{1}{2}\rho\|v_{\text{air}}\|^2$$

$$(2) \quad m = \|v_{\text{air}}\|/v_{\text{sound}}$$

Vehicle squared airspeed ($\|v_{\text{air}}\|^2$) is obtained as the dot product of the air velocity with itself. Note that error due to

wind mismodeling is insignificant when compared to likely error in predicted atmospheric density.

Note that Mach number is needed only in order to obtain reference values of vehicle aerodynamic coefficients, as will be discussed presently. Fortunately, the aerodynamic coefficients of the K-1 OV are very insensitive to errors in Mach number for Mach numbers greater than 2 (almost all the controlled reentry, since a drogue parachute will be deployed and control will be inactive below Mach 2). Thus, rather large error in computing Mach number is acceptable.

Dynamic pressure is used to compute the α -oscillation frequency, as will be discussed below. It will be seen that our design performance is insensitive to errors in Q of 10 to 20 percent.

Nominal Aerodynamic Coefficient Database

Tables of nominal aerodynamic coefficients, parametrized by Mach number (m) and total angle of attack (α^*), are included in the "mission load" database. The primary tabulated quantities are the normal and axial aerodynamic force coefficients C_N and C_A and the longitudinal (x) coordinate of the aerodynamic center of pressure (x_{cp}). Initial data for these tables are from wind tunnel testing. Nominal tables of the partial derivatives with respect to α of these three quantities are included in the database. Partial derivatives are used only in computing the α -oscillation frequency.

Current values of x_{cp} , C_N , and C_A and of the derivatives $x_{\text{cp},\alpha}$, $C_{N,\alpha}$, and $C_{A,\alpha}$ are computed using 2-dimensional linear interpolation in the respective mission-loaded tables. Mach number (m) and total angle of attack (α^*) used in this interpolation are the values computed above.

Modeling the Oscillation in Angle of Attack and Estimation of Trim Alpha

To damp the natural oscillation in angle of attack, the controller must null the vehicle pitch rate at the instant when angle of attack is equal to its trim (zero moment) value. To implement this strategy, the controller requires an estimate of α_{trim} . So as not to use fuel damping an oscillation with amplitude that is insignificant, an estimate of the oscillation amplitude is also needed.

Note that for each Mach number (m), the nominal value of trim angle of attack (α_{trim}) may be obtained by solving for α in the pitch torque balance equation

$$(3) \quad C_N(m,\alpha)[x_{\text{cp}}(m,\alpha) - x_{\text{cg}}] + C_A(m,\alpha)z_{\text{cg}} = 0$$

Here x_{cg} and z_{cg} denote the roll and yaw coordinates of the vehicle center of mass. We hold m fixed and vary α , using interpolation in tables of x_{cp} , C_N , and C_A to determine their corresponding values at α .

Although this method allows us to tabulate α_{trim} vs m in advance, there are several reasons why we prefer to estimate α_{trim} in flight for use by control:

1. The solution to the torque balance equation is rather sensitive to errors in the aerodynamic coefficients. Values of these coefficients available from wind tunnel testing may differ significantly from values experienced in flight. Nominal α_{trim} may therefore be seriously in error.
2. The current angle of attack (α) we compute from vehicle air velocity is incorrect because of EGL misalignment and because of wind errors. If the controller is to act when $\alpha = \alpha_{trim}$, it would be best if the α_{trim} we compare contained similar errors (i.e., onboard estimation of α_{trim} will serve to compensate the effect of errors in α).
3. Some type of onboard estimation is needed to determine α -oscillation amplitude.

Thus, the controller design includes a function to estimate current α_{trim} and to estimate the amplitude of the α -oscillation.

A classical approach is sufficient for this application: we model the α -oscillation as simple harmonic motion of angular frequency Ω about an equilibrium point that is to be estimated. This idea leads to a (slowly time-varying) 3-state linear filter. A natural set of state variables is:

- x_1 = equilibrium position (estimated deviation from nominal α_{trim})
- x_2 = current displacement from equilibrium (estimated $\alpha - \alpha_{trim}$)
- x_3 = derivative with respect to time of x_2 (scaled to nondimensionalize)

The state dynamics has the form

$$\dot{x} = Ax + bu$$

$$(4) \quad y = c'x$$

where u is external forcing (pitch torque N_{jets} due to jet firings plus pitch component of the $-\omega \times I\omega$ Euler coupling from the body rate vector ω).

With appropriate scaling of x_3 , the 3 by 3 matrix A is given by

$$(5) \quad A = \begin{bmatrix} 0 & 0 & 0 \\ 0 & 0 & -\Omega \\ 0 & \Omega & 0 \end{bmatrix}$$

and b is of the form

$$(6) \quad b = \begin{bmatrix} 0 \\ 0 \\ b_3 \end{bmatrix}$$

where $b_3 = -1 / (\Omega I_{2,2})$.

The oscillation angular frequency Ω is computed using dynamic pressure Q and nominal aerodynamics coefficients and their derivatives. Thus

$$(7) \quad C_{m,\alpha} = C_{N,\alpha} [x_{cp} - x_{cg}] + C_N x_{cp,\alpha} + C_{A,\alpha} z_{cg}$$

$$\Omega^2 = -Q S C_{m,\alpha} / I_{2,2}$$

Observation matrix c' is for observation y taken to be the difference of measured α from nominal trim value of α . With the state variables chosen, it follows that

$$(8) \quad c' = [1 \ 1 \ 0]$$

The state equations for the trim estimator are formed from this model in the usual way

$$(9) \quad \dot{x} = Ax + bu + L(y - c'x)$$

With such an implementation, the required estimate of α_{trim} is just the state variable x_1 plus the nominal value of x_{trim} .

The α -oscillation amplitude (M) is readily obtained from the estimator state variables

$$(10) \quad M^2 = x_2^2 + x_3^2$$

The 3 by 1 gain vector (L) can be chosen using any of various well-known methods. For simplicity and robustness, we choose L (which depends on the frequency Ω) using pole placement methods. Since our choice of state variables is "nondimensional," it is appropriate to compute gains $L(\Omega)$ for oscillation frequency Ω by rescaling gains for $\Omega = 1$, i.e.

$$(11) \quad L(\Omega) = \Omega L(1)$$

Viewed as a "black box" single-input single-output system – (observe α , output α_{trim}) – the estimator transfer function has the form

$$(12) \quad H(s) = [1 \ 0 \ 0] (sI - (A - Lc'))^{-1} L$$

It is useful to consider the Bode plot of the design. The frequency response has the following characteristics:

1. Unity gain at $s = 0$ (α_{trim} is found by averaging α).
2. Near zero gain at $s = \pm i\Omega$ (we notch out the anticipated oscillation).

Note that we model the oscillation frequency (Ω) using nominal, imperfectly known aerodynamic coefficients. To reduce sensitivity to error in nominal Ω , we impose the following requirement on the gain set L :

1. Estimator gain must be at least -20 dB at frequencies within $\pm 50\%$ of Ω .

Figure 2 shows the frequency response of the estimator design (normalized to the case $\Omega = 1$).

AERODYNAMIC BANK MANEUVER CONTROL

The primary function of the EC mode is the accurate implementation of the bank angle and bank rate commands from the OV guidance system received each guidance cycle (1 Hz). The EC controller operates at 25 Hz. Guidance provides a target bank angle (ϕ_{NC}) and a signed maneuver rate ($\dot{\phi}_{NC}$) to EC. The overall objective is to construct a maneuver profile to accomplish this bank instruction, while simultaneously maintaining the critical aerodynamic conditions, the angle of attack (α), and the side-slip (β).

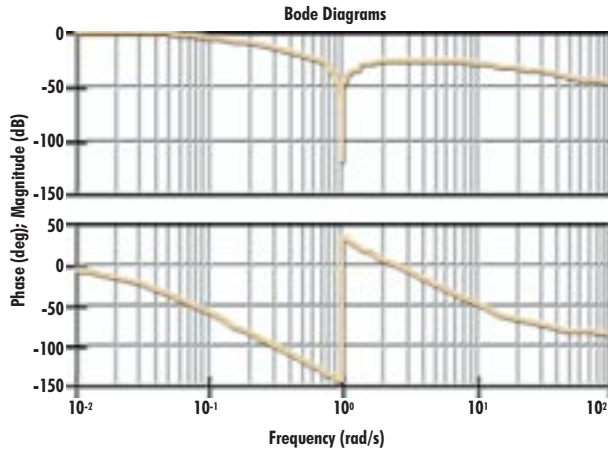


Figure 2 Estimator frequency response

Figure 3 depicts the bank angle as well as the angle of attack and side-slip as defined in the K-1 OV body-fixed reference frame. The actual angle of attack and the side-slip are measured with respect to the wind relative velocity direction, (V_{rel}).

The cumulative angle of attack (α^*), which is the angle between the vehicle x (roll) axis and the V_{rel} , is also depicted in Figure 2. The target aerodynamic configuration of the vehicle is such that the angle of attack and side-slip are at the trim point (α_{trim} and β_{trim}). Note that the α_{trim} is generated by the EC estimator and β_{trim} is assumed equal to 0 here. Hence, the target velocity vector, V_{targ} , is defined as the zero side-slip velocity, the relative velocity that would result if the angle of attack was precisely at α_{trim} and the side-slip was exactly zero. The normalized version of this target velocity, expressed in the body frame, is computed as

$$(13) \quad \hat{V}_{targ} = [\cos(\alpha_{trim}), 0, \sin(\alpha_{trim})]$$

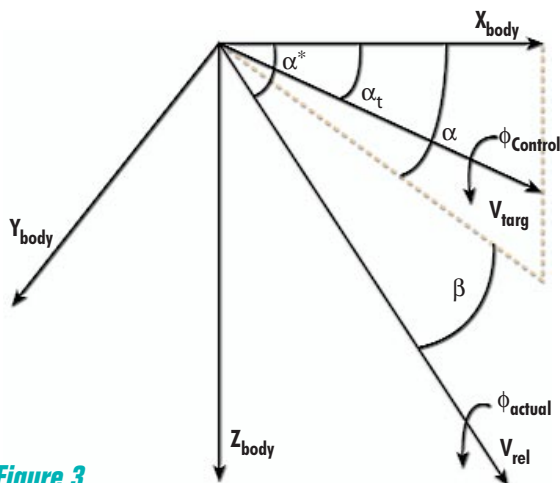


Figure 3 Aerodynamic angles on the K-1 OV

and is used by the EC system as the desired rotation axis for the bank maneuvers. Hence

$$(14) \quad \hat{u}_\phi = \hat{V}_{targ}$$

The control system constructs bank maneuvers by applying the commanded delta-bank angle about the bank rotation axis \hat{u}_ϕ .

Determination of Signed Delta-Bank Angle

Determining the correct signed delta-bank angle is a critical component of the EC's ability to achieve the desired effect on the vehicle's return trajectory. The algorithm must evaluate correctly not only the target bank angle, but also the target maneuver direction. Since the guidance bank and bank rate commands are based only on the previous and current bank angle commands, and since it is, in general, unrealistic to presume that the controller will exactly attain the desired bank angles, there is a risk of the EC misinterpreting the intended direction for the maneuver. Such a scenario is depicted in Figure 4. Suppose the commanded and actual bank state are as shown in the figure. Here, ϕ_{NC} and $\dot{\phi}_{NC}$ are the new commanded bank angle and bank rate just received from guidance, $\phi_{current}$ is the current actual bank angle (as described above), and ϕ_{oc} is the previous valid bank angle command from guidance. Guidance provides a desired bank rate based on the current and previous bank angle commands.

Hence, if the guidance objective is simply to go from ϕ_{oc} to ϕ_{NC} , the short way, then the sign of $\dot{\phi}_{NC}$ will be positive. Given the location of the *actual* bank angle $\phi_{current}$, however, this commanded rate would result in the controller constructing a very large bank maneuver. The integrated effect of such an erroneous maneuver, in terms of the time profile of the vehicle lift vector, must be avoided. Similarly, again with reference to Figure 4, if guidance had intended to perform a large maneuver by traveling from ϕ_{oc} to ϕ_{NC} the long way, then the sign of would be negative. This rate

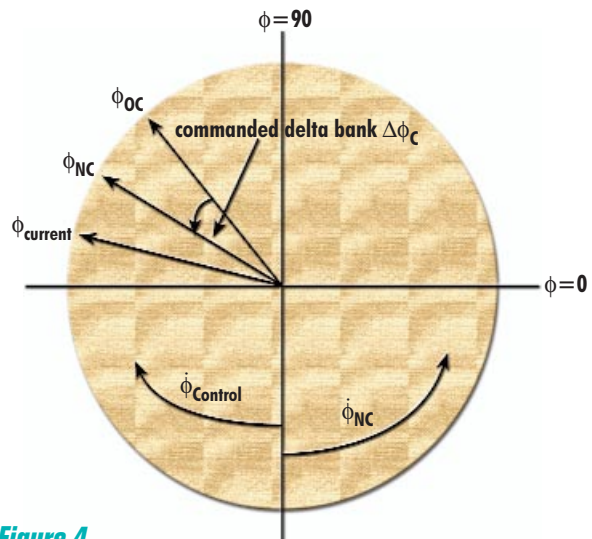


Figure 4 Bank angle direction ambiguity

suggests that control would simply travel the short way from ϕ_{current} to ϕ_{NC} , again potentially resulting in undesirable effects. Hence, under certain conditions, the controller must be intelligent enough to defy the direction commanded by the guidance bank maneuver rate and ascertain what the true objective of the current commands is, based on the current and previous commands as well as the actual bank angle.

Computation of Target Rotation Vectors

Once the correct delta-bank (Δ_ϕ) angle is computed, the current rotation vector for the desired bank maneuver may be constructed. As described above, the rotation axis for the bank maneuver is given by Eq. (14). Therefore, the rotation vector for the bank is simply

$$(15) \quad \vec{\phi} = \Delta_\phi \hat{u}_\phi$$

This will produce roll and yaw maneuvers only, since as shown in Figure 3, the target bank maneuver is about an axis in the body x-z plane. The current vehicle side-slip (β) is computed in the aerodynamic angle computations within EC. The desired side-slip is $\beta_{\text{targ}} = 0$. There are several reasons for this. First, the baseline configuration for the K-1 OV provides a center-of-mass (COM) offset that is along only the body z axis (this offset is largely responsible for the OV having a nonzero trim angle of attack, resulting in controllability). Since the vehicle stability characteristics are such that the aerodynamic torques tend to cause the COM to remain on the side of the vehicle facing the relative velocity vector, it would be inefficient from a fuel perspective to attempt to hold a different β_{targ} . In addition, the K-1 OV is thermally enhanced on the side of the vehicle corresponding to $\beta = 0$. Holding a different side of the vehicle into the wind would risk damage from heat exposure.

To control the side-slip condition in EC, it is shown in Figure 3 that β , like ϕ , is a roll/yaw rotation. Therefore, corrections to account for a nonzero side-slip error are computed as follows

$$(16) \quad \begin{aligned} \vec{\beta} &= (\beta)(K_\beta)[- \sin(\alpha), 0, \cos(\alpha)] \\ \dot{\vec{\beta}} &= (\beta)(K_{\dot{\beta}})[- \sin(\alpha), 0, \cos(\alpha)] \end{aligned}$$

where

- $\vec{\beta}$ = side-slip angle correction vector
- $\dot{\vec{\beta}}$ = side-slip rate correction vector
- K_β = gain on side-slip angle correction
- $K_{\dot{\beta}}$ = gain on side-slip rate correction

Note the actual angle of attack is used in these computations. Equations (15) and (16) provide the extent of the attitude corrections required for roll and yaw maneuvers. The side-slip corrections, given by Eq. (16), are complete in that they are provided in this form to the calculation of total roll/yaw attitude and rate errors (a sum of side-slip and bank errors) for the phase plane logic. The bank vector given by Eq. (15), however, is executed most efficiently by first resolving the total maneuver into individual segments.

Construction of Bank Maneuver Segments

If the total angular error associated with the target bank angle is greater than a database threshold, a bank maneuver will be constructed that results in the classic three-segment ramp-up, coast, ramp-down sequence. Figure 5 depicts a typical maneuver structure, listing the critical angles and rates associated with each segment.

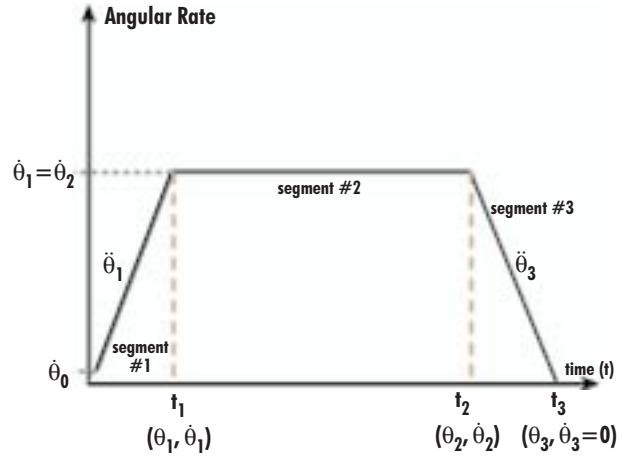


Figure 5
Maneuver structure for control segments

The commanded bank angle and rate from guidance are first validated to ensure that the rate is reasonable for the proposed angular changes in roll and yaw. The minimum required travel for the commanded rate is given by

$$(17) \quad \Delta\theta_{\text{req}} = \left| \frac{\dot{\theta}_{\text{coast}}^2}{\ddot{\theta}_{\text{man}}} \right|$$

where the $\ddot{\theta}_{\text{man}}$ is the nominal expected acceleration capability from the jets. If the desired $\Delta\theta$ is smaller than this minimum, a new maneuver rate is computed as

$$(18) \quad \dot{\theta}_{\text{coast}} = \left\{ \left| \frac{(\Delta\theta)(\ddot{\theta}_{\text{man}})}{(1+K_\theta)} \right| \right\}^{1/2}$$

Note this logic is applied both to the roll portion as well as to the yaw portion of the maneuver. The rotation vector of Eq. (15) is simply resolved into roll and yaw parts and the axes are processed individually. Here, K_θ is a database gain that represents the ratio of coast (segment #2) duration (Δt_2) to acceleration (segment #1) duration (Δt_1). Then, nominal maneuver segments can be constructed using the adjusted maneuver rate, from above, the nominal control acceleration, and the desired angular change. For example, the nominal first (acceleration) segment of the maneuver is described in Eq. (19) using a simple quadratic model. Here, θ_1 is the total angle change from maneuver start to t_1 , at the end of segment #1. Also, $\dot{\theta}_1$ is the rate at the end of segment #1 and $\ddot{\theta}_1$ is the acceleration during segment #1. The initial angular rate is given by $\dot{\theta}_0$.

$$\begin{aligned}
\dot{\theta}_1 &= \left| \dot{\theta}_{\text{coast}} \right| \text{sign}(\Delta\theta) \\
\ddot{\theta}_1 &= \left| \ddot{\theta}_{\text{man}} \right| \text{sign}(\dot{\theta}_1 - \dot{\theta}_0) \\
\Delta t_1 &= \left| \frac{(\dot{\theta}_1 - \dot{\theta}_0)}{\ddot{\theta}_1} \right| \\
(19) \quad \theta_1 &= \dot{\theta}_0(\Delta t_1) + \frac{1}{2} \ddot{\theta}_1 \Delta t_1^2
\end{aligned}$$

Similar computations can be accomplished for the coast segment (#2) and the deceleration segment (#3).

Using the anticipated durations for the three segments in both roll and yaw, computed as in Eq. (19), the coast rates and acceleration magnitudes are potentially adjusted again so that a maneuver coordinated in roll and yaw is designed. This is done by ensuring that the start and end times of each of the maneuver segments are the same for both axes. This feature is necessary to minimize the perturbations to the trim condition that result from performing a bank maneuver. In particular, an uncoordinated bank would result in a temporary increase in the side-slip error. The resulting coast segment rates ($\dot{\theta}_1$) and segments #1 and #3 acceleration values ($\ddot{\theta}_1$ and $\ddot{\theta}_3$) are now used to propagate the target attitudes and rates for the maneuver.

Computation of Velocity Tracking Rates

The velocity tracking rate (VTR) routine computes the effective angular rate of the bank vector ($\dot{\theta}_{\text{VCR}}$) and the angular rate of the air-relative velocity vector ($\dot{\theta}_V$). These are vectors that are computed in the inertial frame and then transformed to the body-fixed frame. The resulting rotational rate vectors are then used in the maneuver design and phase plane error computations to cause the vehicle to track the inertial motions of the bank and velocity vectors. This provides superior controller performance during flight phases where vehicle accelerations are high, rendering the nominal bank maneuver design approach insufficient for tracking the required state. The velocity vector rate is simply the angular motion of the velocity vector, resulting from inertial forces acting on the velocity vector, as seen in the vehicle frame. The bank vector rate is the angular motion of the vector formed by the cross product of inertial velocity and position, resulting from inertial forces acting on this vector, as seen in the vehicle frame.

The procedure is to compute the "tangential" portion of the acceleration vector, which directly influences the effective rotational rate of the air-relative velocity vector. Similarly, we compute the "tangential" component of the vector representing the time-rate-of-change of the bank vector (vcr_I).

First, compute the cross product of velocity and acceleration in the inertial frame and its magnitude

$$\begin{aligned}
v_{\text{mag}} &= \|v_I\|_2 \\
\text{vca}_I &= v_I \times a_I \\
(20) \quad \text{vca}_{\text{mag}} &= \|\text{vca}_I\|_2
\end{aligned}$$

Now, compute the tangential portion of the acceleration vector and its magnitude

$$\begin{aligned}
a_{I_t} &= \text{vca}_I / v_{\text{mag}} \\
(21) \quad a_{t_{\text{mag}}} &= \|a_{I_t}\|_2
\end{aligned}$$

The bank vector in inertial space (vcr_I) and its time derivative are given by

$$\begin{aligned}
\text{vcr}_I &= v_I \times r_I \\
\text{vcr}_{\text{mag}} &= \|\text{vcr}_I\|_2 \\
(22) \quad \text{acr}_I &= \frac{d}{dt}(\text{vcr}_I) = a_I \times r_I
\end{aligned}$$

The tangential portion of the "acr" vector and its magnitude are

$$\begin{aligned}
\text{vcrcacr}_I &= \text{vcr}_I \times \text{acr}_I \\
\text{vcrcacr}_{\text{mag}} &= \|\text{vcrcacr}_I\|_2 \\
\text{acr}_{I_t} &= \frac{\text{vcrcacr}_I}{\text{vcr}_{\text{mag}}} \\
(23) \quad \text{acr}_{t_{\text{mag}}} &= \|\text{acr}_{I_t}\|_2
\end{aligned}$$

Using the components of the time derivatives "tangential" to the velocity and bank vectors, we can write the effective angular rates of the velocity and bank vectors and construct the corresponding rate vectors in inertial and then body frame.

Here, the magnitude of the velocity vector rate and the bank vector rate is

$$\begin{aligned}
\dot{\theta}_{V_{\text{mag}}} &= \frac{a_{t_{\text{mag}}}}{v_{\text{mag}}} \\
(24) \quad \dot{\theta}_{\text{VCR}_{\text{mag}}} &= \frac{\text{acr}_{t_{\text{mag}}}}{\text{vcr}_{\text{mag}}}
\end{aligned}$$

Constructing the corresponding rate vectors in the inertial frame

$$\begin{aligned}
\dot{\theta}_{V_I} &= \dot{\theta}_{V_{\text{mag}}} \left[\frac{\text{vca}_I}{\text{vca}_{\text{mag}}} \right] \\
(25) \quad \dot{\theta}_{\text{VCR}_I} &= \dot{\theta}_{\text{VCR}_{\text{mag}}} \left[\frac{\text{vcrcacr}_I}{\text{vcrcacr}_{\text{mag}}} \right]
\end{aligned}$$

Finally, transform the velocity and bank rate vectors from the inertial frame to the body frame so that they may be incorporated into the controller phase plane rate error computations. Here, ${}_B T_I$ represents the direction cosine matrix, which transforms a vector expressed in inertial space to the equivalent one expressed in body-fixed space.

$$\begin{aligned}
\dot{\theta}_V &= \dot{\theta}_{V_B} = [{}_B T_I] [\dot{\theta}_{V_I}] \\
(26) \quad \dot{\theta}_{\text{VCR}} &= \dot{\theta}_{\text{VCR}_B} = [{}_B T_I] [\dot{\theta}_{\text{VCR}_I}]
\end{aligned}$$

Computation of Angle and Rate Errors

The angle and rate errors associated with the bank maneuvers as well as the side-slip maintenance are computed by simply differencing the target angles and rates and the

actual angles and rates. In the case of the bank maneuvers, the target angles represent the amount of rotation remaining in the current maneuver. This is quantified by propagating a target rotation angle (θ_d) representing the desired amount of remaining rotation (in the particular axis) at the current time into the maneuver (t_{man}), using the nominal control acceleration ($\ddot{\theta}_{man}$) and any initial rate (ω_{old}). Similarly, the target angular rate ($\dot{\theta}_d$) is propagated using $\ddot{\theta}_{man}$ and t_{man} . Once the current maneuver segment is identified, the target angles and rates may be computed. The segment #1 targets are

$$\begin{aligned} \theta_d(i) &= \bar{\theta}_{old}(i) - t_{man}(i)[\omega_{old}(i)] - t_{man}^2(i)[1/2\ddot{\theta}_1(i)] \\ (27) \quad \dot{\theta}_d(i) &= \omega_{old}(i) + t_{man}(i)[\ddot{\theta}_1(i)] \end{aligned}$$

A similar calculation is done for segment #2 (coast), in Eq. (28). Note that the bank rate component ($\dot{\theta}_{VCR}$) is included in the target rates for this segment as it is desired that the commanded rate for the maneuver be supplemented by the residual rate of the bank vector. In other words, it is desired that the vehicle always track the $\dot{\theta}_{VCR}$ rate, whether in a maneuver or not. If in a maneuver, this rate is in addition to the target maneuver rate. It is not included in the target angle profile, however, since the actual rotation rate of the bank vector should completely compensate for the rate supplement, resulting in "0" net angular effect on the rotation vector.

$$\begin{aligned} \theta_d(i) &= \theta_1(i) - [\dot{\theta}_2(i)] [t_{man}(i) - t_1(i)] \\ (28) \quad \dot{\theta}_d(i) &= [\dot{\theta}_2(i)] + \dot{\theta}_{VCR}(i) \end{aligned}$$

The segment #3 targets are similar and include the $\dot{\theta}_{VCR}$ rates as well.

Once the segment number and target angles and rates are known, the errors may be calculated. The angle errors are computed as follows

$$\begin{aligned} \theta'_\epsilon(i) &= \theta_d(i) - \bar{\theta}(i) \\ (29) \quad \theta_\epsilon(i) &= K_\phi(i)[W_\theta(i)(\theta'_\epsilon(i))] - \bar{\beta}(i) \end{aligned}$$

and the rate errors are computed as

$$(30) \quad \dot{\theta}_\epsilon(i) = K_\dot{\phi}(i)[\omega(i) - \dot{\theta}_d(i)] - \dot{\bar{\beta}}(i) - \dot{\theta}_{VCR}(i)$$

The angle errors are computed as the difference between the desired amount of *remaining rotation* for a particular point in the maneuver (θ_d) less the actual amount of rotation remaining for that point in the maneuver ($\bar{\theta}$), supplemented with appropriate side-slip errors ($\bar{\beta}$). The rate error is computed as the difference between the actual rate and the target rate ($\dot{\theta}_d$) supplemented with the corresponding side-slip error rates ($\dot{\bar{\beta}}$). Additionally, the rate of the velocity vector ($\dot{\theta}_V$) is incorporated into the overall rate error to aid in anticipating side-slip motion. The gains (K_ϕ and $K_{\dot{\phi}}$) and the weighting factor (W_θ) are used to prioritize the individual components of the errors.

Phase Plane Processing

The attitude and rate errors are computed using the above methods and are then sent to the phase plane logic to generate the appropriate rotation command vector (R_{CMD}). The detailed processing of the phase plane logic employed in the K-1 system can be found in Ref. [1]. Figure 6 depicts the basic structure of the upper half of the phase plane. The x-axis of the phase plane is the attitude angle error and the y-axis is the attitude rate error. The S1, S2, S3, S4, and S5 are switch curves that dictate the control action. The S1 and S2 curves are derived from general phase plane theory supplemented with attitude deadbands. They are a function of the estimated control acceleration capability for the particular axis. The S3 curve represents the rate error limits and the S4 curve defines the drift channel. The drift channel, as well as S5 defining region 5, are used to minimize propellant use. No firings occur while in region 5 or in the drift channel. Generally, appropriate jet firings will occur while the phase point is in region 1 and region 3, and firings may occur while in region 2. The primary objective is to drive the rate errors $\dot{\theta}_\epsilon$ in a direction of opposite polarity of the angle errors θ_ϵ . The magnitude of the target rate error depends on the magnitude of the angle error. The lower half of the phase plane is essentially the mirror image of the upper half, offset along the x-axis to allow access to region 5 from outside the hysteresis region. The output of the phase plane is the rotation command vector, R_{CMD} , which describes the polarity (+1,-1,0) of the required angular impulse.

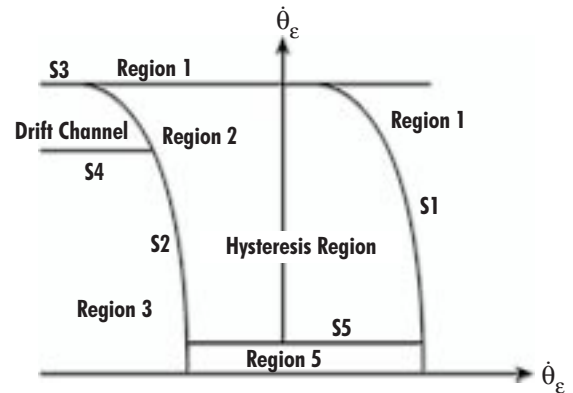


Figure 6 Basic phase plane structure (upper half)

Pitch-Axis Control

The nature of the entry aerodynamics is such that controlling the pitch axis requires different considerations from those of the roll and yaw axes. The pitch control routine is responsible for control decisions for the vehicle pitch axis only. The module generates near-optimal pitch axis commands intended to dissipate undesired kinetic energy. The objective is to minimize angle-of-attack (α) deviations from the trim condition (α_t) while tracking the vehicle's trajectory curvature. Depending on current flight conditions,

the algorithm takes one of four different approaches, as shown in Figure 7. The four different control strategies are:

1. Phase plane control (PPC).
2. Bank coupling control (BCC).
3. Kinetic energy control (KEC).
4. Idle pitch control (IPC).

The current active control approach is indicated in a control status variable.

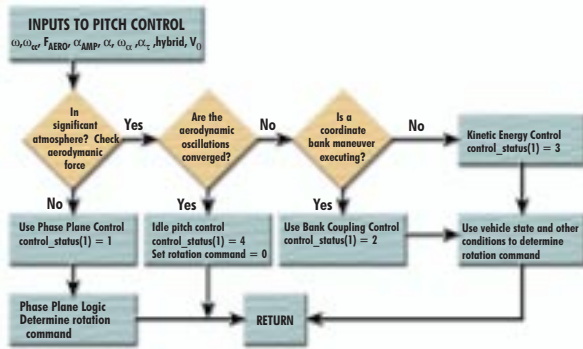


Figure 7
Pitch control high-level logic flow

The first step in the routine is to determine if PPC is appropriate. In the early stages of reentry, the pitch rate and attitude may be controlled by simple phase planes, as described in the previous section. PPC is used whenever the aerodynamic axial force ($F_{AERO}(0)$) is determined to be less than a predetermined threshold (F_{ENTRY}). A low aerodynamic axial force indicates that the current aerodynamic forces do not have a significant effect on the dynamics of the vehicle, thereby allowing the vehicle sufficient control authority to attain an arbitrary pitch rate or angle. When this occurs, the routine sets the control status to "1" and calls the phase plane logic. The desired attitude is the current α_t and the desired rate is that necessary to maintain the trajectory curvature. Hence, the attitude and rate errors for the phase planes are computed as

$$\theta_e = (\alpha - \alpha_t)$$

$$(31) \quad \dot{\theta}_e = \omega(1) - \dot{\theta}_V(1)$$

Note the inclusion of the $\dot{\theta}_V$ term, from the VTR computation to track the rotating velocity. In Eq. (31), $\omega(1)$ is the current actual pitch rate. If it has been determined that the vehicle is currently in significant atmosphere, the next check is to evaluate if the aerodynamic oscillations have attained the converged condition. If they have converged, then no control action is taken ($R_{CMD}(1) = 0$). Also, status is set to IPC (Eq. (4)). Otherwise, the algorithm must determine the particular control phase necessary to best damp the kinetic energy of the system.

If the vehicle is in significant atmosphere but the oscillations have not converged, the algorithm determines if a

coordinated bank maneuver is being accomplished currently. When the vehicle enters a coordinated bank, coupling effects from the roll and yaw axes may have a significant effect on the angle-of-attack motion. In order to prevent these coupling effects from accumulating, the algorithm applies a simple approach to offsetting the kinetic energy imparted on the pitch axis by the cross coupling. The coupling results in a pitch acceleration that could increase the angle of attack and excite a larger aerodynamic oscillation. This effect is countered by first integrating the estimated energy transferred into pitch by the Euler coupling

$$(32) \quad \Delta E_{CC} = \int \ddot{\theta}_{CC} I_{YY} \omega_Y dt$$

where the coupling acceleration is

$$(33) \quad \ddot{\theta}_{CC} = \frac{-1}{I_{YY}} \left[-I_{YZ} \omega_X \omega_Y + I_{XY} \omega_Y \omega_Z + (I_{XX} - I_{ZZ}) \omega_X \omega_Z + I_{XZ} (\omega_Z^2 - \omega_X^2) \right]$$

This is then compared with the amount of energy that potentially could be removed by a control firing

$$(34) \quad \Delta E_C = \ddot{\theta}_C I_{YY} \omega_Y dt$$

In the above equations, I_{YY} is the (2,2) component of the inertia tensor; ω_X , ω_Y , and ω_Z are the current roll, pitch, and yaw body rates, and $\ddot{\theta}_C$ is the nominal expected control acceleration, in this case for the pitch axis. When the accumulated energy change from Eq. (32) exceeds that from Eq. (34), a jet firing is commanded that opposes the existing pitch rate. In this manner, the effects of Euler coupling on the angle-of-attack oscillation are essentially canceled.

SIMULATION RESULTS

The attitude control system design described in the previous text was implemented in a high-fidelity simulation, the K-1 IVS, at Draper. The simulation uses aerodynamic models and vehicle configuration characteristics obtained from Kistler Aerospace. The results presented here are from a "nominal" simulation run. In particular, the environment included no unknown wind conditions, resulting in perfect knowledge of the air-relative velocity vector, perfectly known mass properties, and a perfect aerodynamics model. That is, the flight software models matched the simulation environment for these parameters. Interestingly, the control system is somewhat insensitive to aerodynamic-related errors, including modeling errors and measurement errors, primarily because of the manner in which the aerodynamic conditions are controlled. Errors in the mass properties of the vehicle will result in added propellant consumption, but are not included here.

Figure 8 shows the commanded bank angle (ϕ_{NC}) vs actual (idealized) bank angle ($\phi_{current}$). The commanded angle is generated by the OV guidance and is represented by the straight, steady lines in the plot. The actual bank plot generally oscillates about the commanded angle, primarily because of limit cycling in the phase plane. Some of this "chatter" may be eliminated by further refining the gains

and phase plane limit parameters, although limitations resulting from jet modeling errors and minimum impulse bits dictate that some deadbanding will persist. The actual bank tracks the command to within the 1-deg deadband, which results in the vehicle hitting the target landing zone. Figure 9 shows the vehicle angular rate profiles. The top plot in Figure 9 shows the roll/yaw rate plots. These are overplotted to highlight the nature of the coordinated bank maneuver accomplished. The roll rates attain the noticeably higher rates during the large maneuvers, approximately 7 deg/s and 10 deg/s, respectively, while the yaw rates, seen inside the roll profiles, attain roughly 2 deg/s only. This is because at a trim angle of attack of roughly 11 deg, the bank rotation axis is predominantly roll. Also, from these plots it is clear that nearly coordinated maneuvers are accomplished. The lower plot of Figure 9 shows the pitch-axis rates. The top plot of Figure 10 is the actual angle of attack (α) overplotted with the estimated trim angle of attack (α_t). During nominal pitch control operation (KEC), the jets will fire only when α is near α_t and the pitch rate (Figure 9) exceeds a specified limit (0.2 deg/s). Hence, in this scenario, very little pitch control is required during much of the run. The lower plot of Figure 10 is the actual side-slip (β) angle. The side-slip is controlled to within the 1-deg deadband, with the only substantial disturbances occurring during the large bank maneuvers (about 300 s and again near 700 s). This is primarily because of Euler coupling effects into the yaw axis. Finally, the total propellant usage is shown in Figure 11. The substantial jumps in fuel occur also during the two large bank maneuvers. Smaller increases are attributable to phase plane limit cycling and any pitch and side-slip control actions that have occurred.

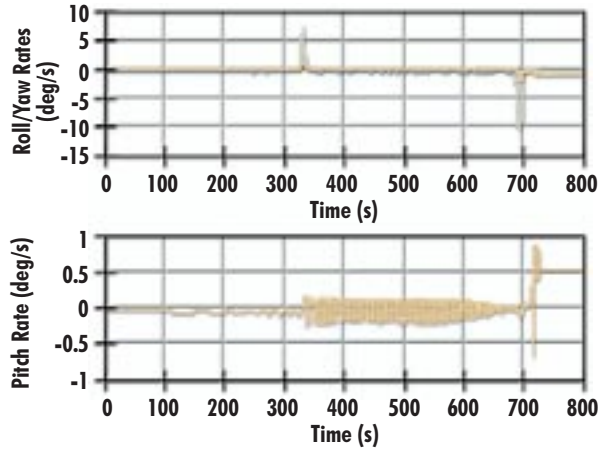


Figure 9
Vehicle angular body rates

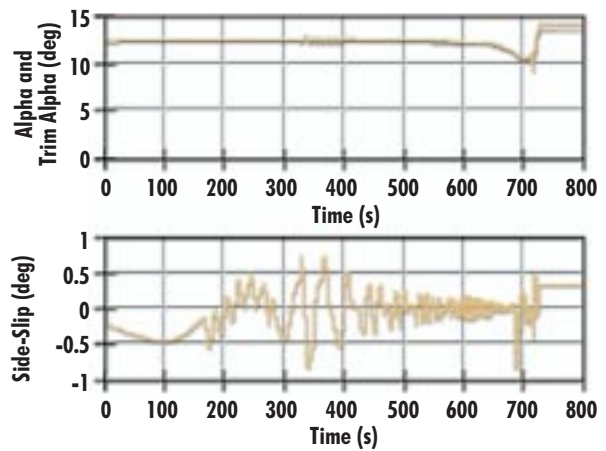


Figure 10
Trim and actual angle of attack and side-slip

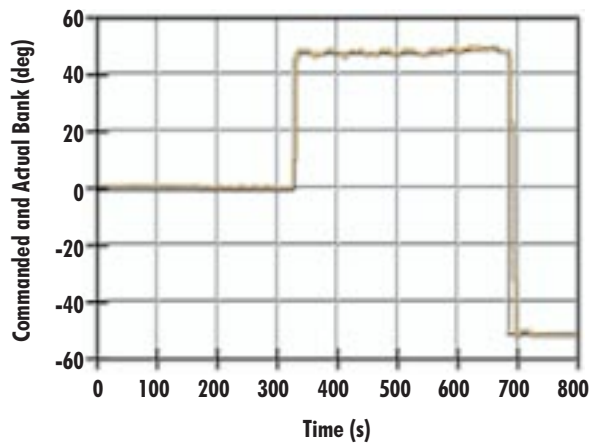


Figure 8
Command bank and actual bank

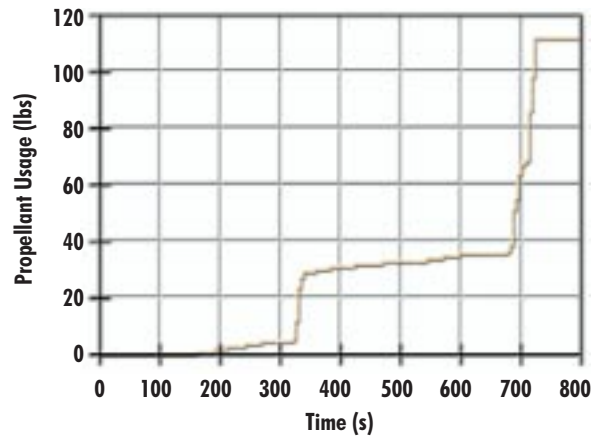


Figure 11
Propellant use

CONCLUSIONS

The design of a system that can successfully control the Kistler K-1 OV from shortly after the completion of a deorbit burn, through atmospheric reentry, and until stabilization parachute deployment has been described. This flight phase lasts less than 15 min, but flight conditions change drastically in this period: altitude goes from greater than 400,000 ft to less than 100,000 ft; Mach number reaches a maximum of greater than 25, and then diminishes until it is less than 2.6; dynamic pressure attains a maximum value greater than 1000 lb/ft². Vehicle angle of attack is controlled to within a fraction of a degree of its trim value for the majority of the reentry trajectory. The vehicle travels more than 4000 mi, while achieving a position error at stabilization parachute deployment typically under 5000 ft. This is largely due to jet commands that control the bank-about-velocity maneuvers and maintain the aerodynamic conditions. This performance is achieved using typically less than 150 lb of propellant.


ACKNOWLEDGMENTS

This work was performed at The Charles Stark Draper Laboratory, Inc., under Contract #191-4000, supported by the Kistler Aerospace Corporation. The contents and ideas presented in this work do not necessarily reflect those of the Kistler Aerospace Corporation.


The authors also wish to thank Draper Laboratory staff members Dr. Michael Ricard and Barry Fink and Draper Laboratory Fellow Robert Bibeau for their technical support and contributions, which made this work possible.

REFERENCES

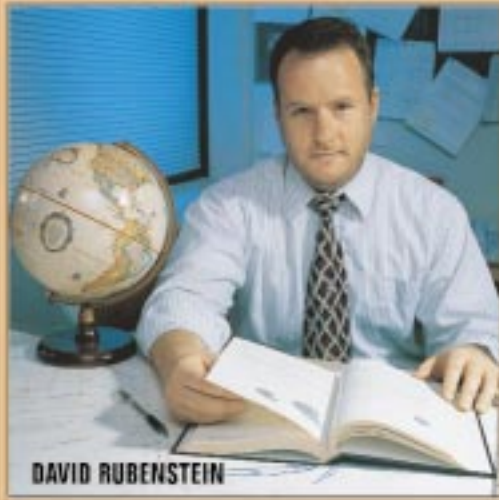
- [1] *Software Requirements Specification for the Flight Manager CSCI of the K-1 Orbital Vehicle*, The Charles Stark Draper Laboratory, Inc., Document No. 318193, Cambridge, MA, May 1998.
- [2] *Apollo Guidance, Navigation and Control*, MIT and The Charles Stark Draper Laboratory, Inc., Technical Software Report R-700, Cambridge, MA, July 1971.
- [3] *Aeroassist Flight Experiment, Attitude Control System Design Book*, MDC91W5015, McDonnell Douglas Space Systems Company, Huntsville AL, June 1991.
- [4] Zacharias, G.L., *A Digital Autopilot for the Space Shuttle Vehicle*, Master of Science Thesis in Aeronautics and Astronautics, Massachusetts Institute of Technology, Cambridge, MA, February 1974.
- [5] Junkins, J.L. and J.D. Turner, *Optimal Spacecraft Rotational Maneuvers*, Elsevier Science Publishing Company, New York, NY, 1986.



BIOGRAPHIES



Attitude Control System Design for Return of the Kistler K-1 Orbital Vehicle



David Rubenstein is a Senior Member of the Technical Staff in the Autonomous Controls Group. Since joining Draper in 1996, he has worked on the design of the Kistler K-1 Vehicle Flight Software as well as associated analysis and simulation, including the incorporation of a flexible-body dynamics model to represent key portions of the K-1 trajectory. He is currently responsible for design and development of the control system for the Best Buy Advanced Technology Demonstration (ATD) vehicle and is also involved in structural modeling for the NASA Space Station and Space Shuttle. Prior to arriving at Draper, Dr. Rubenstein spent seven years at Martin Marietta in Denver, Colorado working on multi-rigid-body satellite dynamics and control and associated ground and flight software issues. His primary interests are in multi-body dynamics, optimization, and optimal control. Mr. Rubenstein received a BS degree in mechanical engineering from Washington University and MS and PhD degrees in aerospace engineering from Pennsylvania State University.

drubenstein@draper.com



David Carter is a Principal Member of the Technical Staff in the Aerospace Control Group. He is interested in algorithms for spacecraft applications and in control and estimation theory. His work since joining Draper Laboratory in 1985 includes estimation algorithm design for the Kistler K-1 vehicle, orbit and momentum control algorithm design for the Hughes HS-702 spacecraft, analysis and simulation of "solar tacking" (use of solar pressure torques) as a satellite momentum control technique, contributions to GPS/INS integration filter design for the A-10 aircraft, and orbit determination accuracy studies for Landsat. He is currently conducting control system analysis for the International Space Station. David received a PhD in mathematics from Columbia University, an MSE in electrical engineering from Princeton, and a BA in physics from Haverford College. Before joining Draper he held the rank of associate professor of mathematics at the University of Virginia.

dcarter@draper.com